

## Size Selective Self-Sorting in Coordination-Driven Self-Assembly of Finite Ensembles

Yao-Rong Zheng, Hai-Bo Yang,\* Brian H. Northrop, Koushik Ghosh, and Peter J. Stang\*

Department of Chemistry, University of Utah, 315 South 1400 East, RM, 2020, Salt Lake City, Utah 84112

Received January 9, 2008

Size selective self-sorting in the coordination-driven self-assembly of two-dimensional (2-D) polygons and three-dimensional (3-D) cages is presented. Two types of polygons (rectangular and triangular) of different size are formed spontaneously from within mixtures of a molecular “clip” or a 60° organoplatinum acceptor with dipyrindyl linkers of different lengths via self-sorting. Furthermore, two different sized 3-D supramolecular cages are formed upon mixing one ditopic organoplatinum acceptor and two different sized tritopic donors from the self-sorting process. The formation of these polygons and cages is characterized using NMR spectroscopy and electrospray ionization mass spectrometry (ESI-MS). In all cases, the self-sorting process is directed by the size of the donor building blocks and a dynamic, thermodynamically driven self-correction process resulting in the formation of discrete products from complex mixtures.

## Introduction

Self-sorting, the mutual recognition of complementary components within a mixture, is a critical phenomenon in many biological systems. When specific information is encoded within the structural aspects of molecular subunits, multiple higher-order supramolecular structures can be obtained from complex, multicomponent mixtures via self-sorting processes.<sup>1</sup> Through detailed investigations of the self-sorting process, valuable insight into analogous biological self-sorting processes may be obtained. Toward this aim, certain pioneering synthetic self-sorting systems based upon metal–ligand coordination bonding,<sup>2</sup> hydrogen bonding,<sup>3</sup> solvophobic effects,<sup>4</sup> and dynamic covalent chemistry<sup>5</sup> have been developed during the past decade.

In the area of synthetic self-sorting systems driven by metal–ligand coordination bonding, Lehn et al. have previously reported the spontaneous formation of discrete supramolecular double helicates in one vessel as directed by the number of binding sites in oligo-bipyridine strands and by the preferred coordination geometry of metal ions.<sup>2a</sup> Raymond et al. later observed self-sorting of supramolecular triple helicates containing two metal centers based solely on

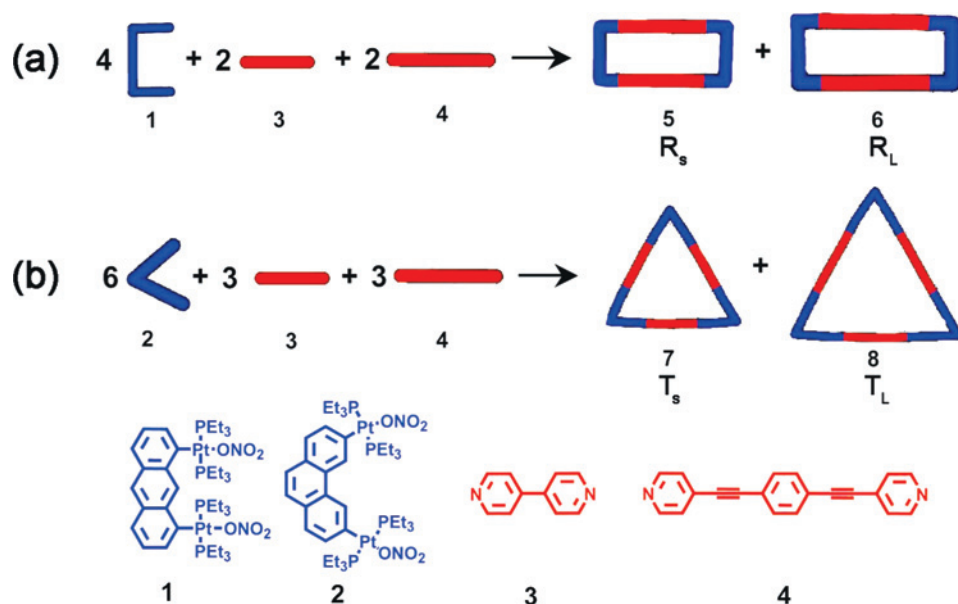
the lengths of rigid spacers separating two catecholate ligands.<sup>2b</sup> Furthermore, self-sorting also can be directed by chiral ligands<sup>2c</sup> and the counteraction of complexes.<sup>2g</sup> However, in contrast to numerous literature reports concerning the self-sorting of helicates, only sporadic studies have been reported on the same process involving self-assembled polygons and polyhedra, which comprise some of the most prominent higher-order structures.<sup>6</sup>

Recently, our group has reported the self-sorting of multiform two-dimensional (2-D) supramolecular polygons via the reaction of a 4,4'-dipyridyl donor with three different organoplatinum acceptors of varying bonding angles.<sup>7</sup> As a result of the structural rigidity and directionality of individual building blocks, the formation of thermodynamically favored

- (2) (a) Krämer, R.; Lehn, J.-M.; Marquis-Rigault, A. *Proc. Natl. Acad. Sci. U.S.A.* **1993**, *90*, 5394. (b) Caulder, D. L.; Raymond, K. N. *Angew. Chem., Int. Ed. Engl.* **1997**, *36*, 1440. (c) Masood, M. A.; Enemark, E. J.; Stack, T. D. P. *Angew. Chem., Int. Ed.* **1998**, *37*, 928. (d) Enemark, E. J.; Stack, T. D. P. *Angew. Chem., Int. Ed.* **1998**, *37*, 932. (e) Stiller, R.; Lehn, J.-M. *Eur. J. Inorg. Chem.* **1998**, 977. (f) Taylor, P. N.; Anderson, H. L. *J. Am. Chem. Soc.* **1999**, *121*, 11538. (g) Albrecht, M.; Schneider, M.; Röttele, H. *Angew. Chem., Int. Ed.* **1999**, *38*, 557. (h) Kondo, T.; Oyama, K.-I.; Yoshida, K. *Angew. Chem., Int. Ed.* **2001**, *40*, 894. (i) Pinalli, R.; Cristini, V.; Sottili, V.; Geremia, S.; Campagnolo, M.; Caneschi, A.; Dalcaneale, E. *J. Am. Chem. Soc.* **2004**, *126*, 6516. (j) Kamada, T.; Aratani, N.; Ikeda, T.; Shibata, N.; Higuchi, Y.; Wakamiya, A.; Yamaguchi, S.; Kim, K. S.; Yoon, Z. S.; Kim, D.; Osuka, A. *J. Am. Chem. Soc.* **2006**, *128*, 7670. (k) Saur, I.; Scopelliti, R.; Severin, K. *Chem. Eur. J.* **2006**, *12*, 1058. (l) Langner, A.; Tait, S. L.; Lin, N.; Rajadurai, C.; Ruben, M.; Kern, K. *Proc. Natl. Acad. Sci. U.S.A.* **2007**, *104*, 17927.

\* To whom correspondence should be addressed. E-mail: hbyang@chem.utah.edu (H.-B.Y.), stang@chem.utah.edu (P.J.S.).

(1) (a) Lehn, J.-M. *Science* **2002**, *295*, 2400. (b) Lehn, J.-M. *Rep. Prog. Phys.* **2004**, *67*, 249. (c) Hollingsworth, M. D. *Science* **2002**, *295*, 2410. (d) Wu, A.; Isaacs, L. *J. Am. Chem. Soc.* **2003**, *125*, 4831.

**Scheme 1.** Graphical Representation of Self-Sorting in the Coordination-Driven Self-Assembly of (a) Supramolecular Rectangles<sup>a</sup> and (b) Triangles<sup>b</sup>


<sup>a</sup> **R<sub>S</sub>**: small rectangle; **R<sub>L</sub>**: large rectangle. <sup>b</sup> **T<sub>S</sub>**: small triangle; **T<sub>L</sub>**: large triangle.

2-D polygons requires, according to the “directional bonding model”,<sup>8</sup> that individual components possessing the same bonding angle undergo self-sorting during the self-assembly process. These studies have been expanded to include three-dimensional (3-D) structures, which generate a series of discrete, highly symmetric 3-D cages in one vessel.<sup>9</sup>

As mentioned above, size, as one essential geometric and directional factor governing self-assembly, has been successfully explored in the self-sorting of helicates.<sup>2b</sup> Very few examples, however, have been reported that involve size selective self-sorting of building blocks during the assembly

of supramolecular polygons or polyhedra. Considering that the final products generated from different sized subunits have the same resultant shape, discriminative selection will likely be more challenging when size is the only information encoded within building blocks during the process of self-sorting of discrete 2-D and 3-D assemblies.

The fundamental question of whether the size differences stored in different molecular components will be able to induce a self-sorting process to generate a highly ordered system of multiple discrete superstructures in a complex mixture is an important one. Herein, we have carried out a study of the self-sorting process in 2-D and 3-D Pt(II) superstructures by mixing different sized ditopic bispyridyl<sup>10</sup> or tritopic trispyridyl donors<sup>11</sup> with a molecular “clip”<sup>10</sup> and 60° acceptor.<sup>12</sup> Despite the possibility of forming myriad oligomeric structures, discrete supramolecular polygons and distorted triangle prisms are strongly preferred in the mixtures, representative of a size selective self-sorting process.

## Results and Discussion

When molecular clip **1** is mixed with two different sized linear bipyridyl linkers **3** (0.72 nm) and **4** (1.65 nm) in a 2:1:1 ratio and heated at 60–65 °C for 45 h in an aqueous acetone solution (v/v 1:1), two molecular rectangles **R<sub>S</sub>** and **R<sub>L</sub>**<sup>10</sup> of different size are formed as the dominant products (Scheme 1a). The self-sorting process was followed by <sup>31</sup>P and <sup>1</sup>H multinuclear NMR spectroscopy as shown in Figures 1 and 2, respectively. After 1 h, the mixture changes from a

- (3) (a) Jolliffe, K. A.; Timmerman, P.; Reinhoudt, D. N. *Angew. Chem., Int. Ed.* **1999**, *38*, 933. (b) Cai, M.; Shi, X.; Sidorov, V.; Fabris, D.; Lam, Y.-F.; Davis, J. T. *Tetrahedron* **2002**, *58*, 661. (c) Corbin, P. S.; Lawless, L. J.; Li, Z.; Ma, Y.; Witmer, M. J.; Zimmerman, S. C. *Proc. Natl. Acad. Sci. U.S.A.* **2002**, *99*, 5099. (d) Ma, Y.; Kolotuchin, S. V.; Zimmerman, S. C. *J. Am. Chem. Soc.* **2002**, *124*, 13757. (e) Wu, A.; Chakraborty, A.; Fettingner, J. C.; Flowers, R. A., II; Isaacs, L. *Angew. Chem., Int. Ed.* **2002**, *41*, 4028. (f) Mukhopadhyay, P.; Zavalij, P. Y.; Isaacs, L. *J. Am. Chem. Soc.* **2006**, *128*, 12098.
- (4) (a) Bilgiclier, B.; Xing, X.; Kumar, K. *J. Am. Chem. Soc.* **2001**, *123*, 11815. (b) Schnarr, N. A.; Kennan, A. J. *J. Am. Chem. Soc.* **2003**, *125*, 667.
- (5) (a) Rowan, S. J.; Hamilton, D. G.; Brady, P. A.; Sanders, J. K. M. *J. Am. Chem. Soc.* **1997**, *119*, 2578. (b) Rowan, S. J.; Reynolds, D. J.; Sanders, J. K. M. *J. Org. Chem.* **1999**, *64*, 5804. (c) Rowan, S. J.; Cantrill, S. J.; Cousins, G. R. L.; Sanders, J. K. M.; Stoddart, J. F. *Angew. Chem., Int. Ed.* **2002**, *41*, 2943. (d) Corbett, P. T.; Leclaire, J.; Vial, L.; West, K. R.; Wietor, J.-L.; Sanders, J. K. M.; Otto, S. *Chem. Rev.* **2006**, *106*, 3652.
- (6) Ziegler, M.; Miranda, J. J.; Andersen, U. N.; Raymond, K. N. *Angew. Chem., Int. Ed.* **2001**, *40*, 733.
- (7) Addicott, C.; Das, N.; Stang, P. J. *Inorg. Chem.* **2004**, *43*, 5335.
- (8) (a) Stang, P. J.; Olenyuk, B. *Acc. Chem. Res.* **1997**, *30*, 502. (b) Leininger, S.; Olenyuk, B.; Stang, P. J. *Chem. Rev.* **2000**, *100*, 853. (c) Seidel, S. R.; Stang, P. J. *Acc. Chem. Res.* **2002**, *35*, 972. (d) Schwab, P. F. H.; Levin, M. D.; Michl, J. *Chem. Rev.* **1999**, *99*, 1863. (e) Holliday, B. J.; Mirkin, C. A. *Angew. Chem., Int. Ed.* **2001**, *40*, 2022. (f) Cotton, F. A.; Lin, C.; Murillo, C. A. *Acc. Chem. Res.* **2001**, *34*, 759. (g) Fujita, M.; Tominaga, M.; Hori, A.; Therrien, B. *Acc. Chem. Res.* **2005**, *38*, 369. (h) Fiedler, D.; Leung, D. H.; Bergman, R. G.; Raymond, K. N. *Acc. Chem. Res.* **2005**, *38*, 349.
- (9) Yang, H.-B.; Ghosh, K.; Northrop, B. H.; Stang, P. J. *Org. Lett.* **2007**, *9*, 1561.

- (10) Kuehl, C. J.; Huang, S. D.; Stang, P. J. *J. Am. Chem. Soc.* **2001**, *123*, 9634.
- (11) Kuehl, C. J.; Kryschenko, Y. K.; Radhakrishnan, U.; Seidel, S. R.; Huang, S. D.; Stang, P. J. *Proc. Natl. Acad. Sci. U.S.A.* **2002**, *99*, 4932.
- (12) Kryschenko, Y. K.; Seidel, S. R.; Arif, A. M.; Stang, P. J. *J. Am. Chem. Soc.* **2003**, *125*, 5193.

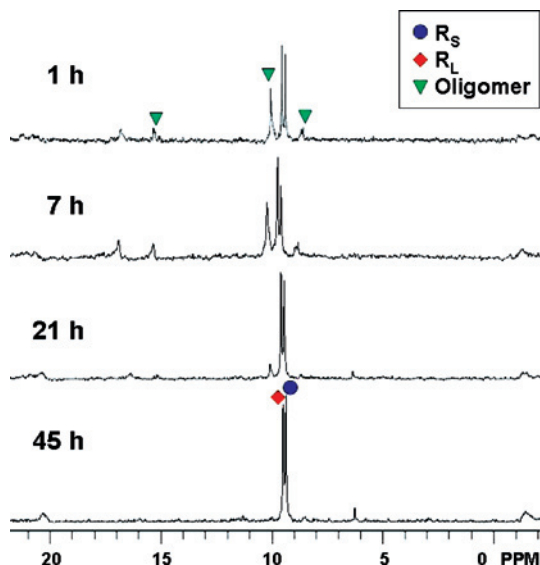


**Figure 1.**  $^{31}\text{P}\{^1\text{H}\}$  NMR spectra (Acetone- $d_6$ /D $_2$ O 1:1) recorded at 1, 7, 21, and 45 h time intervals during the formation of supramolecular rectangles  $\mathbf{R}_S$  and  $\mathbf{R}_L$ .

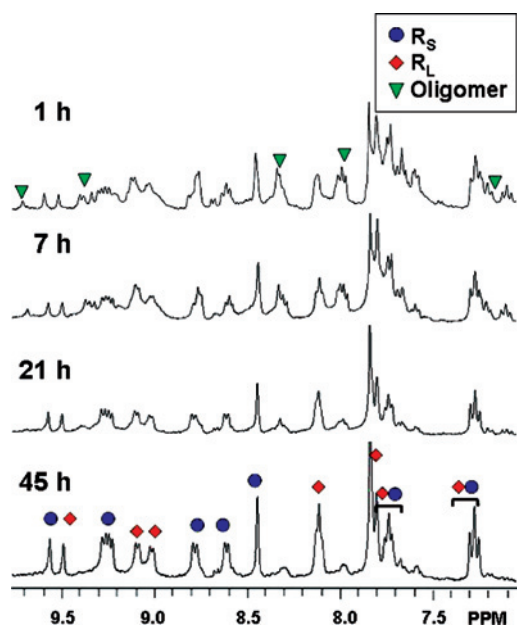


**Figure 2.** Partial  $^1\text{H}$  NMR spectra (Acetone- $d_6$ /D $_2$ O 1:1) recorded at 1, 7, 21, and 45 h time intervals during the formation of supramolecular rectangles  $\mathbf{R}_S$  and  $\mathbf{R}_L$ .

suspension to a clear solution. The  $^{31}\text{P}\{^1\text{H}\}$  NMR spectrum of this reaction mixture shows intense peaks at 8.95 ppm and 9.10 ppm with concomitant  $^{195}\text{Pt}$  satellites for  $\mathbf{R}_S$  and  $\mathbf{R}_L$ , flanked by unassignable signals that are representative of oligomeric byproducts. Likewise, peaks attributable to rectangles  $\mathbf{R}_S$  and  $\mathbf{R}_L$  (e.g.,  $\delta = 9.52$  ppm,  $\text{H}_9$  in  $\mathbf{R}_S$ ;  $\delta = 9.45$  ppm,  $\text{H}_9$  in  $\mathbf{R}_L$ ) can be found in the  $^1\text{H}$  NMR spectrum after 1 h of heating, though broad peaks and unassignable signals belonging to oligomeric byproducts are also observed. After 21 h, the broad byproduct peaks at 7.89 ppm, 8.22 ppm, 9.30 ppm, and 9.64 ppm have decreased significantly while the intense peaks for  $\mathbf{R}_S$  and  $\mathbf{R}_L$  remain in the  $^1\text{H}$  NMR spectrum, indicating that most oligomeric byproducts have dynamically self-sorted to the desired products. After 45 h, two sets of sharp signals (consistent with those previously

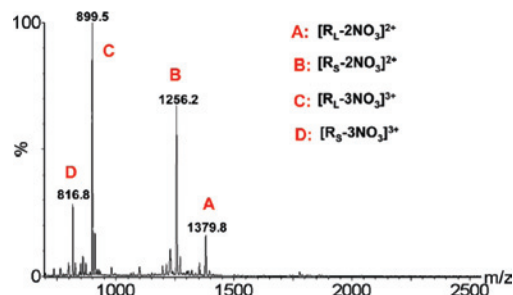


**Figure 3.** Full ESI mass spectrum (Acetone- $d_6$ /D $_2$ O 1:1) of the product mixture containing supramolecular rectangles  $\mathbf{R}_S$  and  $\mathbf{R}_L$ .

reported<sup>10</sup> for  $\mathbf{R}_S$  and  $\mathbf{R}_L$ ) remain in the NMR spectrum, indicating the presence of two highly symmetric Pt(II) supramolecular species obtained as the predominant products in the solution.

The formation of the desired supramolecular rectangles is further confirmed by ESI mass spectrometry as shown in Figure 3. The ESI mass peaks corresponding to the consecutive loss of nitrate anions from the small rectangle  $\mathbf{R}_S$ ;  $m/z = 1256.2$  [ $\text{M} - 2\text{NO}_3$ ] $^{2+}$  and  $m/z = 816.8$  [ $\text{M} - 3\text{NO}_3$ ] $^{3+}$  are observed, as are those corresponding to the formation of the large rectangle,  $\mathbf{R}_L$ , at  $m/z = 1379.8$  [ $\text{M} - 2\text{NO}_3$ ] $^{2+}$  and  $m/z = 899.5$  [ $\text{M} - 3\text{NO}_3$ ] $^{3+}$ . All of these peaks were isotopically resolved and agree with their theoretical distribution, as shown in Figure 4.

The combined evidence from the  $^1\text{H}$  and  $^{31}\text{P}$  NMR spectroscopy as well as ESI mass spectrometry clearly indicate the formation of two discrete molecular rectangles  $\mathbf{R}_S$  and  $\mathbf{R}_L$ , composed of *four* subunits each, from a complex mixture according to a dynamic self-sorting process. To further study such size selective self-sorting processes in the self-assembly of 2-D Pt(II)-based supramolecular systems, another self-sorting system was investigated by mixing 60° di-Pt(II) acceptor **2** with linear linkers **3** and **4**, with the desired supramolecular triangles ( $\mathbf{T}_S$ , small triangle,<sup>12</sup> and  $\mathbf{T}_L$ , large triangle<sup>13</sup>) being composed of *six* subunits each as shown in Scheme 1b.

Heating an aqueous acetone solution (v/v 1:1) containing 60° di-Pt(II) acceptor **2** and two dipyriddy linkers **3** and **4** in a 2:1:1 ratio for 65 h results in the formation of two discrete molecular triangles  $\mathbf{T}_S$  and  $\mathbf{T}_L$  as the main products. The  $^{31}\text{P}\{^1\text{H}\}$  NMR (Supporting Information, Figure S1) of the reaction mixture shows sharp peaks at 15.19 ppm ( $\mathbf{T}_S$ ) and 15.27 ppm ( $\mathbf{T}_L$ ). Two sets of signals corresponding to  $\mathbf{T}_S$  and  $\mathbf{T}_L$  are clearly presented in the  $^1\text{H}$  NMR spectrum (Supporting Information, Figure S2) as well. Signals indicative of minor impurities can, however, be observed in the NMR spectrum even after prolonged heating. ESI mass spectrometry (see Supporting Information) provides further evidence for the formation of the discrete two different sized triangles. The ESI mass spectrum exhibits peaks at  $m/z = 1916.1$  and  $m/z = 927.1$ , corresponding to [ $\text{M} - 2\text{NO}_3$ ] $^{2+}$  and [ $\text{M} - 4\text{NO}_3$ ] $^{4+}$  for  $\mathbf{T}_S$  as well as peaks at  $m/z = 2102.2$  and  $m/z = 1019.8$ , corresponding to [ $\text{M} - 2\text{NO}_3$ ] $^{2+}$  and [ $\text{M}$

(13) The supramolecular triangle  $\mathbf{T}_L$  has been characterized by  $^{31}\text{P}$  and  $^1\text{H}$  multinuclear NMR spectroscopy and ESI mass spectrometry, which are shown in Supporting Information.

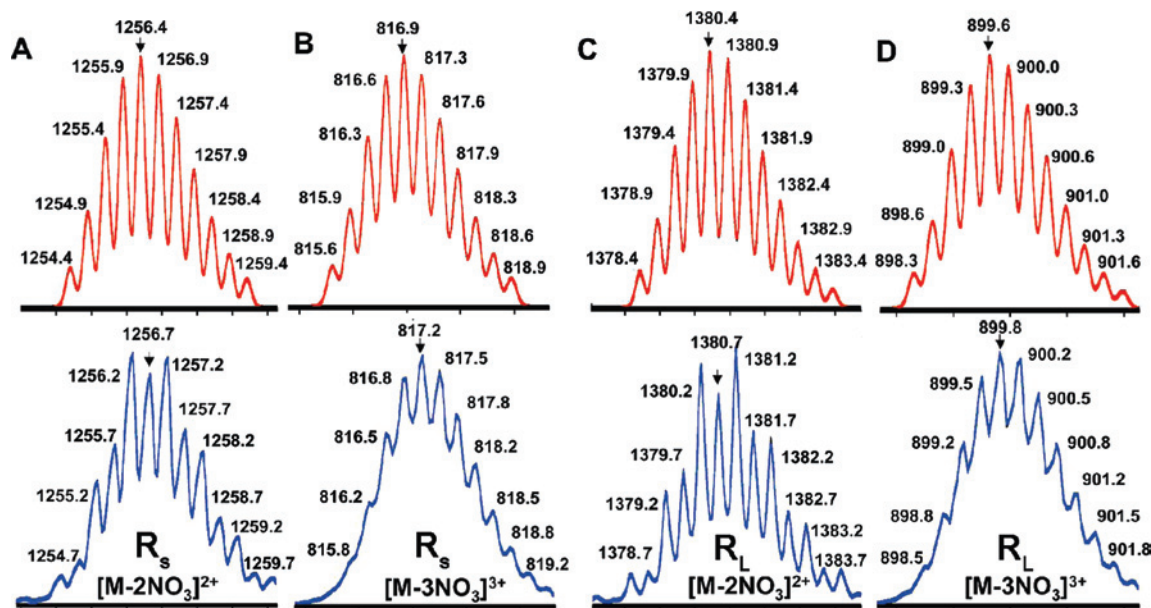
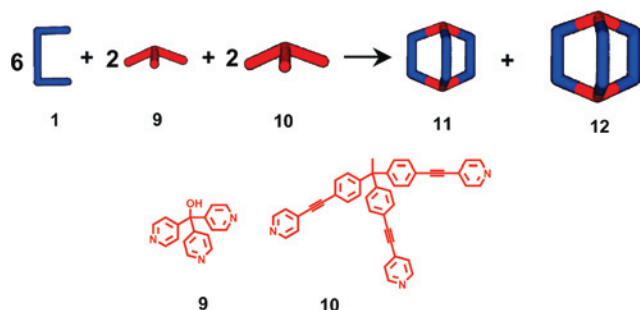


**Figure 4.** Calculated (top, red) and experimental (bottom, blue) ESI mass spectrum (Acetone- $d_6$ /D $_2$ O 1:1) of the product mixture containing supramolecular rectangles  $R_S$  (A and B) and  $R_L$  (C and D).

**Scheme 2.** Graphical Representation of Self-Sorting in the Coordination-Driven Self-Assembly of Supramolecular Distorted Triangular Prisms 11-12



–  $4NO_3$ ] $^{4+}$  for  $T_L$ . All peaks were isotopically resolved and are in agreement with their theoretical distributions.

The collective experimental and analytical data clearly indicate that the formation of different 2-D polygons of the same shape but different size can be achieved from a complex mixture via the self-sorting process. Beyond the 2-D polygons, self-sorting of self-assembly of 3-D supramolecular structures will likely be more challenging as the self-assembly of discrete superstructures is always in competition with oligomerization. Hence, it is even more interesting to determine whether this strategy can be successfully employed to prepare different sized 3-D structures with same shape from multiple components in one pot. The investigation of size selective self-sorting in the self-assembly of 3-D structures was thus carried out by mixing molecular clip **1** with two tritopic donors **9** and **10** in a 6:2:2 ratio as shown in Scheme 2. Analysis of the mixture using multinuclear NMR  $^{31}P$  and  $^1H$  spectroscopy (Figures 5 and 6, respectively) and ESI mass spectrometry (Figures 7 and 8) show that the distorted triangular prisms  $DTP_S$  (small distorted triangular prism) and  $DTP_L$  (large distorted triangular prism) $^{11}$  were formed as the predominant species in the aqueous acetone solution (acetone- $d_6$ /D $_2$ O 1:1) after heating at 70 °C for 24 h.

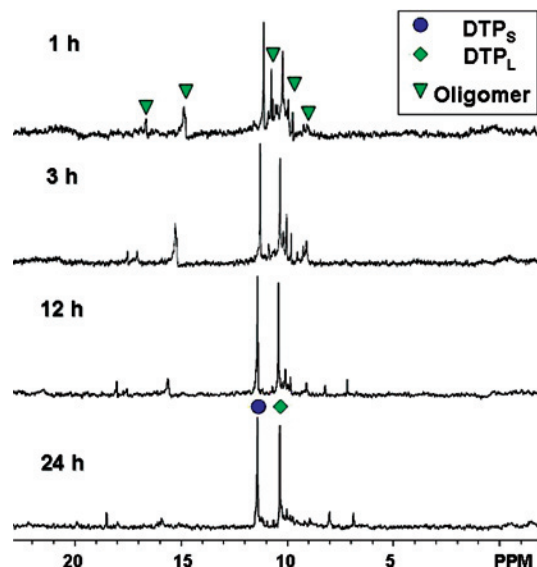


**Figure 5.**  $^{31}P\{^1H\}$  NMR spectra (Acetone- $d_6$ /D $_2$ O 1:1) of recorded at 1, 3, 12, and 24 h time intervals during the formation of distorted triangular prisms  $DTP_S$  and  $DTP_L$ .

The mixture changes from a suspension to a clear solution after 1 h, though highly disordered  $^{31}P\{^1H\}$  and  $^1H$  NMR spectra are observed. After 3 h, initial formation of  $DTP_S$  and  $DTP_L$  is clearly indicated by the  $^{31}P\{^1H\}$  NMR spectrum, where two peaks at 11.12 ppm and 10.16 ppm with concomitant  $^{195}Pt$  satellites for  $DTP_S$  and  $DTP_L$  appeared. There exist, however, multiple unassignable peaks, such as those at 15.31 ppm, 9.85 ppm, and 8.87 ppm, that are representative of oligomeric byproducts in the solution. At the 3 h time interval, signals for  $DTP_S$  and  $DTP_L$  cannot be identified in the  $^1H$  NMR spectrum because of the breadth of peaks corresponding to the oligomeric byproducts. After 12 h, peaks attributable to discrete  $DTP_S$  and  $DTP_L$  can be identified in both the  $^{31}P\{^1H\}$  NMR spectrum and the  $^1H$  NMR spectrum, as the intensities of peaks corresponding to

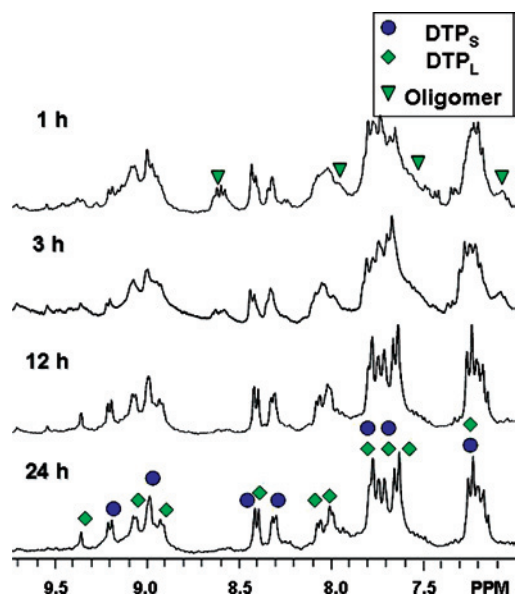


**Figure 6.** Partial  $^1\text{H}$  NMR spectra (Acetone- $d_6$ / $\text{D}_2\text{O}$  1:1) recorded at 1, 3, 12, and 24 h time intervals during the formation of distorted triangle prisms  $\text{DTP}_\text{S}$  and  $\text{DTP}_\text{L}$ .

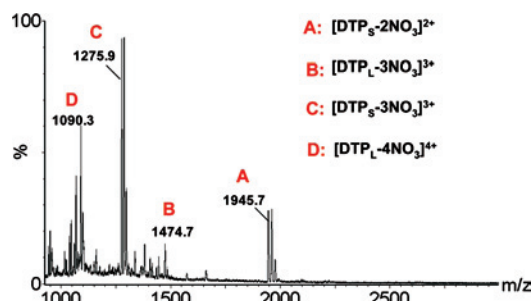


**Figure 7.** Full ESI mass spectrum (Acetone- $d_6$ / $\text{D}_2\text{O}$  1:1) of product mixture containing distorted triangular prisms  $\text{DTP}_\text{S}$  and  $\text{DTP}_\text{L}$ .

oligomeric byproducts are significantly decreased. After 24 h, in the  $^{31}\text{P}$   $\{^1\text{H}\}$  and  $^1\text{H}$  NMR spectra, clearly identifiable peaks as shown in Figures 5 and 6 reveal the formation of two different sized discrete supramolecular 3-D cages  $\text{DTP}_\text{S}$  and  $\text{DTP}_\text{L}$  as the major self-sorted species in the solution.

ESI mass spectrometry (Figure 7) confirms the formation of the different sized supramolecular 3-D cages  $\text{DTP}_\text{S}$  and  $\text{DTP}_\text{L}$  in the mixture. The ESI mass peaks corresponding to the consecutive loss of nitrate anions from the small cage  $\text{DTP}_\text{S}$  at  $m/z = 1946.0$  [ $\text{M} - 2\text{NO}_3$ ] $^{2+}$  and  $m/z = 1276.5$  [ $\text{M} - 3\text{NO}_3$ ] $^{3+}$  are observed, as are those corresponding to the formation of the large cage  $\text{DTP}_\text{L}$  at  $m/z = 1474.5$  [ $\text{M} - 3\text{NO}_3$ ] $^{3+}$  and  $m/z = 1090.4$  [ $\text{M} - 4\text{NO}_3$ ] $^{4+}$ . All peaks were isotopically resolved and agree with their theoretical distribution, shown in Figure 8.

During the self-sorting processes described above, the difference in size of either ditopic donors **3** and **4** or tritopic donors **9** and **10**, in cooperation with other structural factors such as the directionality and rigidity of all donors and acceptors, directs the exclusive formation of the desired discrete superstructures **5–8** and **11–12** from within complex mixtures. Indeed, the thermodynamic stability of different products plays a significant role in this size directing self-sorting process.<sup>10</sup> Closed systems are preferred enthalpically, as they contain at least one more coordination bond than

related open analogues of the same size. Entropic driving forces<sup>2b</sup> favor the formation of multiple, discrete rectangles or triangles as the smallest close system over the formation of oligomeric byproducts. Oligomeric, kinetic intermediate products are formed early in the self-assembly process via random combinations of building blocks. However, these oligomeric structures can be self-sorted, leading to discrete, stable supramolecular ensembles as the kinetically labile Pt–N bond enables a dynamic self-correction process to take place. Hence, this thermodynamically driven self-correction results in the exclusive formation of multiple discrete supramolecular entities from the early oligomeric byproducts in the mixture, whereby size selective self-sorting is achieved.

In conclusion, we have demonstrated that ditopic organoplatinum acceptors **1** or **2**, when mixed with two different sized dipyridyl linkers **3** and **4** or tritopic donors **9** and **10**, undergo a self-sorting process that results in the formation of discrete 2-D or 3-D superstructures. The observed self-sorting systems rely on the thermodynamic preferences (enthalpic and entropic) of the supramolecular ensembles, whereby the size of the linkers can direct the self-selection. These results also help provide an enhanced understanding of the control variables that regulate the self-sorting process and have implications in the related processes that govern the assembly of more complex biological structures in nature.

## Experimental Section

**Methods and Materials.** Building Blocks **1**,<sup>10</sup> **2**,<sup>12</sup> **4**,<sup>10</sup> **9**,<sup>11</sup> and **10**<sup>11</sup> were prepared according to literature procedures. Deuterated solvents were purchased from Cambridge Isotope Laboratory (Andover, MA). NMR spectra were recorded on a Varian Unity 300 spectrometer. The  $^1\text{H}$  NMR chemical shifts are reported relative to residual solvent signals, and  $^{31}\text{P}$  NMR resonances are referenced to an external unlocked sample of 85%  $\text{H}_3\text{PO}_4$  ( $\delta$  0.0). Mass spectra for **R**<sub>S</sub>, **R**<sub>L</sub>, **T**<sub>S</sub>, **T**<sub>L</sub>,  $\text{DTP}_\text{S}$ , and  $\text{DTP}_\text{L}$  were recorded on a Micromass Quattro II triple-quadrupole mass spectrometer using electrospray ionization with a MassLynx operating system.

**Self-Sorting of Rectangles.** Molecular “Clip” **1** (4.44 mg, 0.00382 mmol), 4,4'-dipyridyl **3** (0.30 mg, 0.0019 mmol), and 1,4-bis(4-pyridylethynyl)benzene **4** (0.53 mg, 0.0019 mmol) were placed in a 2-dram vial, following by adding 0.8 mL of a mixture of solvent (Acetone- $d_6$ / $\text{D}_2\text{O}$  1:1), which was then sealed with Teflon tape and immersed in an oil bath at 60–65 °C for 45 h. The yellow orange solution was periodically transferred to an NMR tube for analysis. After two sets of signals corresponding to **R**<sub>S</sub> and **R**<sub>L</sub> were clearly present in the NMR spectra with no further changes, the reaction mixture was characterized by ESI/MS.  $^1\text{H}$  NMR (Acetone- $d_6$ / $\text{D}_2\text{O}$ : 1/1, 300 MHz). For **R**<sub>S</sub>:  $\delta$  9.53 (s, 2H, H<sub>9</sub>), 9.21 (d,  $^3J = 5.8$  Hz, 4H, H $_{\alpha\text{-Py}}$ ), 9.18 (d,  $^3J = 5.4$  Hz, 2H, H $_{\alpha'\text{-Py}}$ ), 8.71 (d,  $^3J = 5.4$  Hz, 4H, H $_{\beta\text{-Py}}$ ), 8.53 (d,  $^3J = 5.4$  Hz, 4H, H $_{\beta'\text{-Py}}$ ), 8.37 (s, 2H, H<sub>10</sub>), 7.71 (d,  $^3J = 10.5$  Hz, 4H, H<sub>4,5</sub>), 7.62 (m, 4H, H<sub>2,7</sub>), 7.14 (t,  $^3J = 7.2$  Hz, 4H, H<sub>3,6</sub>), 1.45 (m, 48H, PCH<sub>2</sub>CH<sub>3</sub>), 0.84 (m, 72H, PCH<sub>2</sub>CH<sub>3</sub>). For **R**<sub>L</sub>:  $\delta$  9.45 (s, 2H, H<sub>9</sub>), 9.03 (d, 4H,  $^3J = 5.1$  Hz, H $_{\alpha\text{-Py}}$ ), 8.95 (d, 4H,  $^3J = 5.4$  Hz, H $_{\alpha'\text{-Py}}$ ), 8.36 (s, 2H, H<sub>10</sub>), 8.03 (m, 8H, H $_{\beta\text{-Py}}$ ), 7.74 (s, 8H, H $_{\text{phenylene}}$ ), 7.71 (d, 4H,  $^3J = 10.5$  Hz, H<sub>4,5</sub>), 7.64 (m, 4H, H<sub>2,7</sub>), 7.14 (t,  $^3J = 7.2$  Hz, 4H, H<sub>3,6</sub>), 1.45 (m, 48H, PCH<sub>2</sub>CH<sub>3</sub>), 0.84 (m, 72H, PCH<sub>2</sub>CH<sub>3</sub>).  $^{31}\text{P}$   $\{^1\text{H}\}$  NMR (Acetone- $d_6$ / $\text{D}_2\text{O}$ : 1/1, 121.4 MHz). For **R**<sub>S</sub>:  $\delta$  8.95 ( $^{195}\text{Pt}$  satellites,  $^1J_{\text{Pt-P}} = 2671$  Hz). For **R**<sub>L</sub>:  $\delta$  9.10 ( $^{195}\text{Pt}$  satellites,  $^1J_{\text{Pt-P}} = 2671$  Hz).

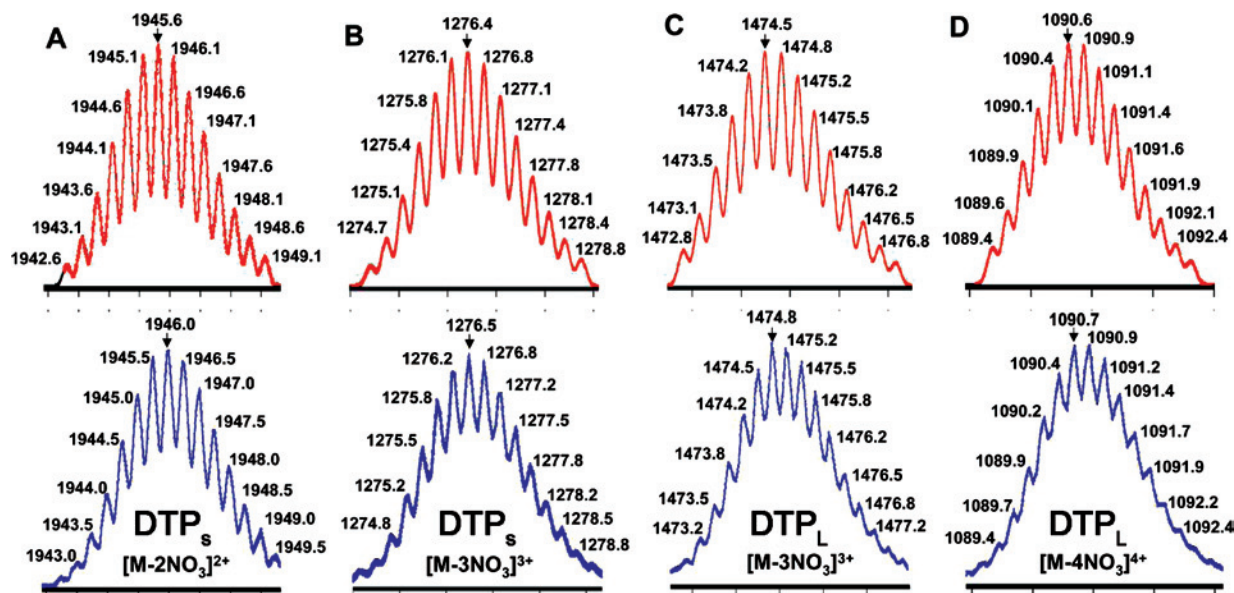


**Figure 8.** Calculated (top, red) and experimental (bottom, blue) ESI mass spectrum (Acetone- $d_6$ /D $_2$ O 1:1) of product mixture containing distorted triangular prisms  $DTP_S$  and  $DTP_L$ .

**Self-Sorting of Triangles.** A 60° organoplatinum acceptor **2** (4.44 mg, 0.00382 mmol), 4,4'-dipyridyl **3** (0.30 mg, 0.0019 mmol), and 1,4-Bis(4-pyridylethynyl)benzene **4** (0.53 mg, 0.0019 mmol) were placed in a 2-dram vial, following by adding 1.4 mL of a mixture of solvent (Acetone- $d_6$ /D $_2$ O 1:1), which was then sealed with Teflon tape and immersed in an oil bath at 60–65 °C for 65 h. After two sets of signals corresponding to  $T_S$  and  $T_L$  were clearly present in the NMR with no further changes, the reaction mixture was characterized by ESI/MS.  $^1H$  NMR (Acetone- $d_6$ /D $_2$ O: 1/1, 300 MHz). For  $T_S$ :  $\delta$  9.11 (d,  $^3J = 5.7$  Hz, 6H,  $H_{\alpha-Py}$ ), 9.06 (d,  $^3J = 5.7$  Hz, 6H,  $H_{\alpha-Py}$ ), 8.62 (s, 6H,  $H_{4,5}$ ), 8.32 (d,  $^3J = 6.3$  Hz, 6H,  $H_{\beta-Py}$ ), 8.29 (d,  $^3J = 6.0$  Hz, 6H,  $H_{\beta-Py}$ ), 7.65 (d,  $^3J = 8.4$  Hz, 6H,  $H_{2,7}$ ), 7.54 (m, 12H,  $H_{1,8,9,10}$ ), 1.30 (m, 72H,  $PCH_2CH_3$ ), 1.07 (m, 108H,  $PCH_2CH_3$ ). For  $T_L$ :  $\delta$  8.87 (m, 12H,  $H_{\alpha-Py}$ ), 8.54 (s, 6H,  $H_{4,5}$ ), 7.80 (d, 12H,  $^3J = 6.6$  Hz,  $H_{\beta-Py}$ ), 7.71 (s, 12H,  $H_{phenylene}$ ), 7.65 (d,  $^3J = 8.4$  Hz, 6H,  $H_{2,7}$ ), 7.54 (m, 12H,  $H_{1,8,9,10}$ ), 1.30 (m, 72H,  $PCH_2CH_3$ ), 1.07 (m, 108H,  $PCH_2CH_3$ ).  $^{31}P$   $\{^1H\}$  NMR (Acetone- $d_6$ /D $_2$ O: 1/1, 121.4 MHz). For  $T_S$ :  $\delta$  15.19 ( $^{195}Pt$  satellites,  $^1J_{Pt-P} = 2639$  Hz). For  $T_L$ :  $\delta$  15.27 ( $^{195}Pt$  satellites,  $^1J_{Pt-P} = 2654$  Hz).

**Self-Sorting of Distorted Triangle Prisms.** Molecular “Clip” **1** (7.92 mg, 0.00681 mmol), tritopic tectons **5** (0.59 mg, 0.0022 mmol), and **6** (1.29 mg, 0.00230 mmol) were placed in a 2-dram vial, following by adding 0.8 mL of a mixture of solvent (Acetone- $d_6$ /D $_2$ O 1:1), which was then sealed with Teflon tape and immersed in an oil bath at 65–70 °C for 24 h. The yellow orange solution was periodically transferred to an NMR tube for analysis. After

two sets of signals corresponding to  $DTP_S$  and  $DTP_L$  were clearly present in the NMR spectra with no further changes, the reaction mixture was characterized by ESI/MS.  $^1H$  NMR (Acetone- $d_6$ /D $_2$ O: 1/1 300 MHz). For  $DTP_S$ :  $\delta$  9.14 (d, 6H,  $^3J = 6.3$  Hz,  $H_{\alpha-Py}$ ), 8.98 (m, 9H,  $H_{\alpha-Py,9}$ ), 8.36 (s, 3H,  $H_{10}$ ), 8.25 (d, 6H,  $^3J = 4.2$  Hz,  $H_{\beta-Py}$ ), 7.72 (m, 12H,  $H_{\beta-Py}$ ,  $H_{4,5}$ ), 7.68 (d, 6H,  $^3J = 9.9$  Hz,  $H_{2,7}$ ), 7.14 (m, 6H,  $H_{3,6}$ ), 1.40 (m, 72H,  $PCH_2CH_3$ ), 0.82 (m, 108H,  $PCH_2CH_3$ ). For  $DTP_L$ :  $\delta$  9.32 (s, 3H,  $H_9$ ), 9.01 (d, 6H,  $^3J = 5.1$  Hz,  $H_{\alpha-Py}$ ), 8.91 (d, 6H,  $^3J = 4.8$  Hz,  $H_{\alpha-Py}$ ), 8.36 (s, 3H,  $H_{10}$ ), 8.00 (d, 6H,  $^3J = 6.0$  Hz,  $H_{\beta-Py}$ ), 7.95 (d, 6H,  $^3J = 6.0$  Hz,  $H_{\beta-Py}$ ), 7.73 (m, 12H,  $H_{4,5,2,7}$ ), 7.57 (d, 12H,  $^3J = 8.4$  Hz,  $H_{3,5-phenylene}$ ), 7.17 (d, 12H,  $^3J = 8.1$  Hz,  $H_{2,6-phenylene}$ ), 7.14 (m, 6H,  $H_{3,6}$ ), 1.40 (m, 72H,  $PCH_2CH_3$ ), 0.82 (m, 108H,  $PCH_2CH_3$ ).  $^{31}P$   $\{^1H\}$  NMR (Acetone- $d_6$ /D $_2$ O: 1/1 121.4 MHz)  $DTP_S$ :  $\delta$  11.12 ( $^{195}Pt$  satellites,  $^1J_{Pt-P} = 2639$  Hz). For  $DTP_L$ :  $\delta$  10.16 ( $^{195}Pt$  satellites,  $^1J_{Pt-P} = 2654$  Hz).

**Acknowledgment.** P.J.S. thanks the NIH (Grant GM-057052) and the NSF (Grant CHE-0306720) for financial support. B.H.N. thanks the NIH (Grant GM-080820) for financial support.

**Supporting Information Available:** NMR and ESI mass spectra of pure  $T_L$  and product mixture  $T_S$  and  $T_L$  (PDF). This material is available free of charge via the Internet at <http://pubs.acs.org>.

IC800038J